

Temporal scale of environmental correlations affects ecological synchrony

Robert A. Desharnais,^{1,2*} Daniel C. Reuman,^{3,4} Robert F. Costantino⁵ and Joel E. Cohen^{6,7,8}

Abstract

Population densities of a species measured in different locations are often correlated over time, a phenomenon referred to as synchrony. Synchrony results from dispersal of individuals among locations and spatially correlated environmental variation, among other causes. Synchrony is often measured by a correlation coefficient. However, synchrony can vary with timescale. We demonstrate theoretically and experimentally that the timescale-specificity of environmental correlation affects the overall magnitude and timescale-specificity of synchrony, and that these effects are modified by population dispersal. Our laboratory experiments linked populations of flour beetles by changes in habitat size and dispersal. Linear filter theory, applied to a metapopulation model for the experimental system, predicted the observed timescale-specific effects. The timescales at which environmental covariation occurs can affect the population dynamics of species in fragmented habitats.

Keywords

Ecological synchrony, environmental correlations, metapopulations, microcosm experiments, Moran effect, population dispersal, spectral analysis, *Tribolium*.

Ecology Letters (2018)

INTRODUCTION

Synchrony is the correlation over time of population densities of a species measured in different locations. Recent studies have shown synchrony's importance for conservation biology, natural resource management, agriculture, and public health. Synchronous outbreaks of pests and pathogens can cause widespread damage (Myers 1990, 1998; Porter *et al.* 1991; Earn *et al.* 1998; Bjørnstad *et al.* 2008; Sheppard *et al.* 2016), and synchrony can negatively affect the persistence of metapopulations (Harrison & Quinn 1989; Heino *et al.* 1997; Earn *et al.* 2000). Spatial covariance in environmental factors and synchrony may be increasing as a result of climate change; examples have been reported for arctic caribou (Post & Forchhammer 2004), boreal forests (Shestakova *et al.* 2016), wintering birds (Koenig & Liebhold 2016), aphids (Sheppard *et al.* 2016) and butterflies (Kahilainen *et al.* 2018).

Several factors cause or enhance synchrony. Spatial correlation in environmental variables that affect population growth can lead to synchrony, a phenomenon known as the 'Moran effect' (Moran 1953; Ranta *et al.* 1997; Hudson & Cattadori 1999). Dispersal of individuals among populations can cause or enhance synchrony (Ranta *et al.* 1995; Haydon & Steen 1997; Ripa 2000; Chevalier *et al.* 2014; Martin *et al.* 2017). Interactions with other synchronous species or synchronous age-classes can also induce synchrony (Liebhold *et al.* 2004;

Ripa & Ranta 2007). Data analysis and modelling have shown that these causal factors of synchrony can interact in complex ways and need to be considered in combination (Bjørnstad *et al.* 1999; Kendall *et al.* 2000; Liebhold *et al.* 2004; Abbott 2007).

Synchrony has been measured several ways. Correlation coefficients characterise the covariance between two time series (Bjørnstad & Falck 2001; Buonaccorsi *et al.* 2001). This approach ignores the possibility that synchrony can vary at different timescales. Some recent studies used spectral methods to measure synchrony at different timescales (Grenfell *et al.* 2001; Vasseur & Gaedke 2007; Keitt 2008; Sheppard *et al.* 2016; Defriez *et al.* 2016; Defriez & Reuman 2017a,b). Timescale-specific approaches have the advantage of using more of the information in time series and sometimes provide insight into the mechanisms that drive synchrony. For example, Sheppard *et al.* (2016) analysed annual time series from 1976 to 2010 for 20 aphid species and used methods based on wavelets to examine which environmental drivers best explained changes in aphid synchrony. They showed that long timescale synchrony in aphid first flights fell from before 1993 to after, and that, in 18 of 20 aphid species, an average of 80% of this synchrony is due to covariance in winter climate. These studies show that the timescales at which synchrony occurs matter for understanding the influence of environmental factors on regional-scale population dynamics.

¹Department of Biological Sciences, California State University at Los Angeles, Los Angeles, CA 90032, USA

²Control and Dynamical Systems, California Institute of Technology, Pasadena, CA 91125, USA

³Department of Ecology and Evolutionary Biology, University of Kansas, Lawrence, KS 66045, USA

⁴Kansas Biological Survey, University of Kansas, Lawrence, KS 66047, USA

⁵Department of Ecology and Evolutionary Biology, University of Arizona, Tucson, AZ 85721, USA

⁶Laboratory of Populations, Rockefeller University, New York, NY 10065, USA

⁷Earth Institute and Department of Statistics, Columbia University, New York, NY 10027, USA

⁸Department of Statistics, University of Chicago, Chicago, IL 60637, USA

*Correspondence: E-mail: rdeshar@calstatela.edu

Controlled experimental studies involving laboratory microcosms can enhance our understanding of ecological phenomena (Jessup *et al.* 2004; Desharnais 2005). Lab studies of synchrony have involved several species including soil mites (Benton *et al.* 2001, 2002), rotifers and algae (Fontaine & Gonzalez 2005), *Drosophila* (Dey & Joshi 2006), maize weevils (Lima-Ribeiro *et al.* 2007), bacteria and bacteriophages (Vogwill *et al.* 2009), *Euplotes* and *Tetrahymena* predator–prey protists (Vasseur & Fox 2009; Fox *et al.* 2011), ciliates and parasitic bacteria (Duncan *et al.* 2015), and phytoplankton (Massie *et al.* 2015). Two of these studies altered the spectral properties of the imposed environmental variation and analysed the effects on total population synchrony. Fontaine & Gonzalez (2005) varied randomly the densities of the algal resource for the rotifers, with one treatment level having dominant frequencies biased towards long timescales and another level having different dominant frequencies of equal power. The presence or absence of dispersal was included as an additional experimental factor. The authors showed that the synchronising effect of dispersal was enhanced in the populations with resource fluctuations biased towards long timescales. Massie *et al.* (2015) varied the autocorrelation of the randomised dilution rates they used in their chemostat experiments and showed that synchrony between phytoplankton populations can, under some circumstances, be enhanced beyond the correlation of the environmental drivers, a phenomenon they called the ‘enhanced Moran effect’.

We use laboratory populations of the flour beetle *Tribolium castaneum* to extend this earlier work in three important ways. We examine how (1) changes in dispersal and in the cospectral properties of the environmental noise affect synchrony, (2) how these changes affect not just total population synchrony, but also its timescale structure, and (3) how filter theory, applied to a linearised version of a mathematical model for the population system, predicts the spectral features of the data. We also provide an extension of Moran’s theorem to the spectral properties of populations synchronised by environmental noise.

MATERIALS AND METHODS

Experimental design

The experimental unit was a metapopulation composed of two vials of flour beetles. Different pairs of vials were manipulated in different ways according to two crossed experimental factors: habitat size fluctuations and adult dispersal. The two levels of the habitat fluctuation factor were imposed with paired random flour volume sequences that were generated to be (1) positively correlated on long timescales (low frequencies) and negatively correlated on short timescales (high frequencies), herein denoted as Low⁺/High⁻ or (2) positively correlated on short timescales and negatively correlated on long timescales, herein High⁺/Low⁻. How the habitat sequences were generated is described later. The two levels of adult dispersal were (1) no dispersal, or (2) a reciprocal exchange of 25% of the adults between populations at each census. There were three replicates for each of the four treatment groups to yield 12 experimental metapopulations containing 24 paired laboratory cultures.

Data were collected from each population every two weeks. At each census t , the number of A-stage (sexually mature adults), P-stage (last instar non-feeding larvae, pupae, and callow adults) and L-stage (feeding larvae) beetles were counted. These numbers are denoted as $A_{t,b}^{(1)}$, $A_{t,b}^{(2)}$, $P_{t,b}^{(1)}$, $P_{t,b}^{(2)}$, $L_{t,b}^{(1)}$, and $L_{t,b}^{(2)}$, where ‘ b ’ represents ‘before manipulation’ and the superscript identifies the first or the second population of the two-vial metapopulation. Additional mortality was imposed upon adults and larvae and adult dispersal was performed using the following equations:

$$A_t^{(i)} = \text{rd}\left((1-d)(1-m_A)A_{t,b}^{(i)}\right) + \text{rd}\left(d(1-m_A)A_{t,b}^{(j)}\right), \quad (1)$$

$$L_t^{(i)} = \text{rd}\left((1-m_L)L_{t,b}^{(i)}\right), \quad (2)$$

for $i, j = 1, 2$, $i \neq j$, where m_L and m_A are the additional imposed larval and adult mortality rates, d is the rate of adult dispersal, and ‘rd’ is the rounding function to the nearest integer. Values of $m_A = 0.05$ and $m_L = 0.70$ were chosen to yield population dynamics characterised by undercompensatory decay to a stable equilibrium based on previous work and assuming a constant habitat size (Dennis *et al.* 2001; Table 1, conditional least squares (CLS) estimates, control group). The adult dispersal rate was either $d = 0.00$ or $d = 0.25$ as determined by the dispersal treatment level. P-stage beetles were not manipulated ($P_t^{(i)} = P_{t,b}^{(i)}$). Each population was maintained in a half-pint (237 mL) milk bottle and kept in a dark incubator at 32 °C. Every two weeks, the life stages were counted, manipulated and the numbers $A_t^{(i)}$, $P_t^{(i)}$, and $L_t^{(i)}$ ($i = 1, 2$) were returned to fresh medium. Eggs were discarded at each census, a practice consistent with previous *Tribolium* experiments (Costantino *et al.* 1995, 1997, 2005; Dennis *et al.* 1995, 2001; Cushing *et al.* 2002). Because the duration of the egg stage is short (2–3 days) compared to the two weeks between successive censuses, these eggs were soon replaced by adult females. Dead adults were removed. This procedure continued for 80 weeks (40 time units). The adult and larval mortality and adult dispersal manipulations were imposed at every census $t > 0$. All populations were initiated with $A_0^{(i)} = 486$, $P_0^{(i)} = 67$, and $L_0^{(i)} = 82$ ($i = 1, 2$), which is close to the predicted deterministic equilibrium for a single model population using the parameter estimates of Dennis *et al.* (2001) cited above, adjusted for the imposed mortality and mean habitat size of the present study.

Habitat fluctuations

We generated a habitat size sequence for each replicate metapopulation as follows. (1) We created an autoregressive first-order time series of length 40 with standard normal marginals and a lag-one autocorrelation coefficient of 0.9 (for red noise) or -0.9 (for blue noise) independently for each replicate. (2) We created a time series of 20 values of -23 g and 20 values of 23 g. (3) We used spectral mimicry (Cohen *et al.* 1999) to permute the time series of step 2 to have spectra similar to that of step 1. Mimicry ensured an equal number of 23’s and -23 ’s. (4) We let s_r (respectively, s_b) equal the series in step 3 that mimics the red (respectively, blue) noise autoregressive process. (5) For the Low⁺/High⁻ habitat regime, we used $s_r + s_b + 54$ g for the habitat sequence of one population and $s_r - s_b + 54$ g for the habitat sequence of the other population. For the High⁺/

Table 1 Numeric measures of synchrony between habitats within metapopulations.

Habitat fluctuations	Dispersal	Frequency range	Synchrony (mean \pm SE)		
			L-stage	P-stage	A-stage
Low ⁺ /High ⁻	$d = 0$	Low	0.138 \pm 0.025	0.141 \pm 0.022	0.678 \pm 0.047
		High	-0.648 \pm 0.056	-0.653 \pm 0.050	-0.065 \pm 0.018
		Total	-0.510 \pm 0.042	-0.511 \pm 0.043	0.612 \pm 0.063
High ⁺ /Low ⁻	$d = 0$	Low	-0.114 \pm 0.027	-0.120 \pm 0.022	-0.726 \pm 0.049
		High	0.522 \pm 0.014	0.497 \pm 0.006	0.017 \pm 0.006
		Total	0.409 \pm 0.041	0.377 \pm 0.024	-0.708 \pm 0.043
Low ⁺ /High ⁻	$d = 0.25$	Low	0.133 \pm 0.013	0.131 \pm 0.014	0.919 \pm 0.028
		High	-0.617 \pm 0.051	-0.616 \pm 0.051	-0.019 \pm 0.002
		Total	-0.483 \pm 0.038	-0.485 \pm 0.037	0.900 \pm 0.030
High ⁺ /Low ⁻	$d = 0.25$	Low	-0.166 \pm 0.008	-0.143 \pm 0.033	0.598 \pm 0.035
		High	0.414 \pm 0.012	0.418 \pm 0.017	0.136 \pm 0.010
		Total	0.248 \pm 0.016	0.275 \pm 0.050	0.734 \pm 0.030

Total synchrony is the Pearson correlation. Synchrony for low- and high-frequency ranges was computed as in Methods. Means and standard errors (SE) are across replicates.

Low⁻ habitat regime, we used $s_r + s_b + 54$ g for the habitat sequence of one population and $-s_r + s_b + 54$ g for the habitat sequence of the other population. Thus, the only amounts of medium used were 8, 54 and 100 g. The bivariate time series used for the habitat fluctuations were synchronised at long (respectively, short) timescales and anti-synchronised at short (respectively, long) timescales.

The mean value of every habitat time series was exactly 54 g and the total correlation of the bivariate habitat time series for each replicate was exactly zero. Under traditional definitions of synchrony in terms of correlation, all experimental replicates experienced unsynchronised noise. Correlation does not reveal the timescale (or, equivalently, frequency-specific) structure of synchrony in the habitat time series we generated. We here and henceforth use the term ‘frequency’ of an oscillatory component of a time series to refer to the reciprocal of the timescale of the oscillation.

Metapopulation *Tribolium* model

We analysed our experiments using a metapopulation version of the lattice stochastic demographic larvae–pupae–adult (M-LSD-LPA) model:

$$L_{t+1,b}^{(i)} = \text{rd} \left(\left[\sqrt{bA_t^{(i)} \exp\left(-\frac{c_{el}}{V_t^{(i)}}L_t^{(i)} - \frac{c_{ea}}{V_t^{(i)}}A_t^{(i)}\right) + E_{1t}^{(i)}} \right]^2 \right), \quad (3)$$

$$P_{t+1,b}^{(i)} = \text{rd} \left(\left[\sqrt{(1-\mu_l)L_t^{(i)} + E_{2t}^{(i)}} \right]^2 \right), \quad (4)$$

$$A_{t+1,b}^{(i)} = \text{rd} \left(\left[\sqrt{P_t^{(i)} \exp\left(-\frac{c_{pa}}{V_t^{(i)}}A_t^{(i)}\right) + (1-\mu_a)A_t^{(i)} + E_{3t}^{(i)}} \right]^2 \right), \quad (5)$$

where $[x]$ is the maximum of 0 and x . Equations (3–5) predict the number of insects of each life stage in population i

of the metapopulation before we impose additional mortality and dispersal; equations (1–2) give the number of insects returned to the medium after a census. The unit of time is two weeks, which is the approximate amount of time spent in both the L stage class and the P stage class under experimental conditions. Parameter b is the average number of larvae recruited per adult per unit time in the absence of cannibalism. The fractions μ_a and μ_l are the adult and larval probabilities, respectively, of dying from causes other than cannibalism in one time-unit. The exponentials represent the fractions of individuals surviving cannibalism in each unit of time, with cannibalism coefficients c_{el} , c_{ea} , and c_{pa} for egg cannibalism by larvae and adults, and pupal cannibalism by adults, respectively. To facilitate comparison of our parameter estimates with previous studies, habitat size, which varies with time, is $V_t^{(i)}$ for population i and has values of the weight of medium divided by 20 g, the amount routinely used in our laboratory. The random variables $E_{1t}^{(i)}$, $E_{2t}^{(i)}$, and $E_{3t}^{(i)}$ simulate demographic noise added on a square root scale and are chosen from a trivariate normal distribution with a diagonal covariance matrix Σ ; they are assumed to have no serial autocorrelations or cross-correlations.

The deterministic metapopulation model (M-LPA) is recovered by setting the random variables to zero and removing the rounding operation from equations (1–5) (SI-§S3.3). The single-population version of this model has been well tested in constant- and varying-volume experiments (Dennis *et al.* 1995, 2001; Costantino *et al.* 1998, 2005; Cushing *et al.* 2002; Henson *et al.* 2002; Desharnais *et al.* 2006; Reuman *et al.* 2006, 2008).

Parameter estimation and confidence intervals

We used conditional least squares (CLS) to estimate parameter values for the M-LSD-LPA model. We simulated the experimental data 2000 times using the M-LSD-LPA model and CLS estimates and re-estimated parameter values from these simulations to obtain confidence intervals for the parameters. Details are provided in SI-§S3.2.

Estimation of experimental spectra, corrspectra, and related statistics

We estimated raw periodograms from the bivariate metapopulation time series of each life stage using the MATLAB function *specpgram.m*, which is a modified version of the *spec.pgram.R* algorithm from R. We obtained spectra and cross-spectra by smoothing the periodograms using a modified Daniell kernel with spans (5, 5), implemented as the MATLAB function *modDaniell.m*. (MATLAB code for both algorithms is available in SI-§S7.) We computed a normalised spectrum, $\tilde{S}_w(f)$, for life stage w as a function of frequency, f , for each population by dividing the estimated spectrum, $S_w(f)$, by its integral from $f=0$ to $f=0.5$. We computed numerical integrals using the trapezoid method. We computed a ‘corrspectrum’, $\tilde{C}_w(f)$, for life stage w by dividing, at every sampled frequency, the cospectrum (real part of the smoothed cross-spectrum), $C_w(f)$, by the square root of the product of the two spectra from the component populations. Thus, the corrspectra are calculated in a manner analogous to the computation of the Pearson correlation coefficient; they represent the cospectral power as a fraction of the geometric mean spectral power of the component time series at each frequency and are bounded so that $-1 \leq \tilde{C}_w(f) \leq 1$ for $f \in [0, 0.5]$. Corrspectra reveal frequency-specific changes in synchrony of a bivariate time series independent of frequency-specific changes in the variances.

We obtained confidence bands for the corrspectra by using the M-LSD-LPA model and CLS parameter estimates to simulate the experimental protocol 2000 times. We generated a new set of random habitat sizes for each simulated experiment. We estimated normalised spectra and corrspectra for each simulated experiment as described above. At each frequency, the 2.5th and 97.5th percentiles of the 2000 corrspectral power estimates yielded 95% confidence intervals.

As a measure of total synchrony, we computed the Pearson correlation coefficient ρ for each life stage in each replicate metapopulation. We used *specpgram.m* to compute the unsmoothed cospectrum, $C_w(f)$, which provided cospectral values at frequencies f_1, f_2, \dots, f_τ . These values are related to the estimated Pearson correlation by the equation

$$\rho = \frac{2}{(N-1)\sigma_1\sigma_2} \sum_{j=1}^{\tau} C_w(f_j), \quad (6)$$

where σ_1 and σ_2 are the estimated standard deviations, N is the length of the paired time series, and τ is the number of corrspectral frequencies. We broke the summation in (6) into separate sums over low ($0 \leq f_j < 0.25$) and high ($0.25 \leq f_j < 0.5$) frequency bands and used these two components to partition the total synchrony, ρ , into long and short timescales, respectively. We chose $f = 0.25$ as a dividing line between low and high frequency bands because one cycle every four time periods is exactly half the Nyquist frequency and because it is a boundary between Fourier components with positive and negative lag-1 autocorrelation (Sheppard *et al.* 2016).

To characterise the timescale dependence of synchrony for each life stage in each metapopulation, we computed the

‘corrspectral slope’ from a linear regression of the corresponding corrspectrum as a function of frequency. Negative values for the corrspectral slope represent synchrony dominated by low frequencies, whereas positive values represent synchrony dominated by high frequencies.

Spectral predictions from linear filter theory

We used the M-LPA model with randomly generated habitat sizes and linear filter theory to derive predictions for the observed population spectra and corrspectra. Substitution of the CLS parameter estimates into the M-LPA model with constant habitat size $V^* = 2.7$ (54 g/20 g) predicts a stable population equilibrium. We viewed the population fluctuations induced by changes in habitat size as random perturbations and used a linearisation of the M-LPA model around the equilibrium to obtain predictions for the normalised spectra and corrspectra. Details are in SI-§S2, §S3, and §S4.

RESULTS

Theoretical predictions for a general metapopulation model

We prove mathematically, for a general model, that changes in timescale-specific environmental correlations will cause changes in timescale-specific synchrony, as well as changes in total synchrony, even when total environmental correlations remain unchanged. Consider a model with two habitat patches,

$$w_i(t) = [c_1 w_i(t-1) + \dots + c_n w_i(t-n) + q_0 \varepsilon_i(t) + \dots + q_m \varepsilon_i(t-m)](1-d) + [c_1 w_j(t-1) + \dots + c_n w_j(t-n) + q_0 \varepsilon_j(t) + \dots + q_m \varepsilon_j(t-m)]d, \quad (7)$$

for $i, j = 1, 2$, $i \neq j$. Here, $w_i(t)$ is the deviation of a population size index, $x_i(t)$, in habitat patch i at time t , from an equilibrium value x_i^* . The parameters c_1, \dots, c_n define intrinsic population dynamics, $0 \leq d < 1/2$ is a dispersal parameter, and $\varepsilon_i(t)$ represents a random environmental variable in patch i at time t . The parameters q_0, \dots, q_m are coefficients for the environmental noise variables. We assume $(\varepsilon_1, \varepsilon_2)$ is a second-order stationary stochastic process with $E(\varepsilon_i) = 0$. We assume that ε_1 and ε_2 are identically distributed and that the oscillations of ε_1 and ε_2 are in phase; that is, the cross-spectrum of $(\varepsilon_1, \varepsilon_2)$ is real. We also assume a stationary stochastic process that solves (7) exists. The model (7) is a linearisation of a general, spatially symmetric, metapopulation model. The linear approximation is good assuming a stable equilibrium and weak noise (SI-§S1.2).

To show how the timescale of correlations in environmental variation affects the timescale-specific structure of synchrony, we refer to *adjustments* (in italics) in the cospectrum of the environmental noise, C_ε , as any changes to it for which the environmental noise spectrum, S_ε , and the covariance of the environmental noise, $\text{cov}(\varepsilon_1, \varepsilon_2)$, remain constant. In SI-§S1, we show that, in general, *adjustments* will affect the population spectra and variance, as well as the metapopulation cospectrum, corrspectrum, covariance and correlation. When there is no dispersal ($d = 0$), the population spectra and variance will

be unaffected by *adjustments* and the population corrpectrum will equal the environmental corrpectrum. This result can be considered a frequency-specific generalisation of the Moran theorem (Moran 1953). With or without dispersal, *adjustments* can result in a total synchrony (population correlation) that exceeds the total environmental correlation. (Numerical examples appear in SI-§S1.1.) The timescale on which environmental correlation occurs affects synchrony above and beyond the effects of total environmental correlation.

Observed and predicted experimental population time series

We now analyse the experimental data in relation to theory. The timescale patterns of synchrony and anti-synchrony are apparent in the bivariate plots of habitat size and population numbers (Fig. 1). For the $Low^+/High^-$ treatments, medium volumes are positively correlated above or below the mean value of 54 g for long periods of time, but on a short timescale they are negatively correlated (Fig. 1a, g). The opposite is true for $High^+/Low^-$ treatments (Fig. 1d, j). The effects of these different patterns of timescale-specific habitat changes can be seen in the way the two population time series for each metapopulation co-vary. In the $Low^+/High^-$ habitat regime, L-stage and A-stage numbers vary synchronously over long timescales, but anti-synchronously over short timescales (Fig. 1b, c, h, i). The converse is true for the insect numbers in the $High^+/Low^-$ habitat regime with one exception: when dispersal is present ($d = 0.25$), adult numbers are synchronous on both the short and long timescales (Fig. 1l).

There are major differences between the immature and adult life stages in the variation of population numbers. The L-stage (and P-stage, SI-§S5) insect numbers oscillate widely on a short timescale while the magnitudes of those oscillations vary over a long timescale. Numbers of adults vary largely over long timescales, while changes in habitat size induced much smaller oscillations over short timescales. The difference arises because cohorts of immatures develop quickly into adults, whereas adults are long-lived. Egg cannibalism by larvae and adults is an important mechanism driving demographic oscillations in the immature life stages of *Tribolium* (Desharnais & Liu 1987), and so high-frequency changes in habitat size driving similar changes in rates of egg-cannibalism can cause rapid changes in immature numbers. Since adults are not subject to cannibalism, the magnitude of changes is limited by the rate of adult mortality, which is small relative to the intercensal period (CLS estimate is $\mu_a = 0.03664$). The result is that immatures are sensitive and adults are insensitive to high frequency changes in habitat size.

We used the CLS parameter estimates and experimental initial conditions in the M-LPA model to predict life-stage time series for each experimental habitat sequence. These predicted time series are generated from initial conditions and the model only, not step by step. Figure 2 shows the predicted values for the same replicates as in Fig. 1. The agreement between the observed and predicted values is remarkable. Even subtle changes in population numbers are usually well predicted by the model. Despite its simplicity, the M-LPA model predicts well population trajectories when habitat size is altered. SI-§S5 shows that the strong predictive value of the M-LPA model extends to all the experimental metapopulations.

The background of these findings is extensive. Cannibalism is an important mechanism of nonlinear population dynamics in *Tribolium* (Costantino *et al.* 1995, 1997; Benoît *et al.* 1998; Dennis *et al.* 2001) and cannibalism rates scale with habitat size (Costantino *et al.* 1998). Observed insect numbers agree well with the LPA model predictions in varied experimental contexts (Cushing *et al.* 2002; Costantino *et al.* 2005).

Spectral results from the experimental populations

Observed life stage spectra and corrpectra

Most of the variation in L-stage numbers occurs at high frequencies whereas most variation in A-stage numbers occurs at low frequencies for all treatment groups (plots of $\tilde{S}_w(f)$, Fig. 3). The corrpectra reflect the properties of experimentally imposed habitat sequences. For the $Low^+/High^-$ habitat regime, the corrpectra of both the L-stages and A-stages shift gradually from strong synchrony at low frequencies to strong anti-synchrony at high frequencies. The opposite trend is seen in the $High^+/Low^-$ habitat regime, except for adults with dispersal (Fig. 3p). Dispersal transformed anti-synchrony at low frequencies into synchrony, flattening the corrpectra. This finding shows that dispersal and the timescale of environmental correlation can interact in their effects on synchrony. It is consistent with the results of Kendall *et al.* (2000) for total population synchrony. They showed that the interaction between environmental correlation and dispersal always exists when both are present, and that the interaction is opposite in sign to the environmental correlation.

Effect of habitat fluctuations and dispersal on population correlations and corrpectra

Table 1 gives the total synchrony and its decomposition into low and high frequency ranges for the L-, P-, and A-stages (Methods). In all cases except one, the total synchrony is the sum of a positive correlation at low frequencies and a negative correlation at high frequencies or vice-versa. The exception is the A-stage when the habitat regime is $High^+/Low^-$ and dispersal links the two populations. In this case, the two populations have positive correlations for both the low- and high-frequency ranges, again indicating that the timescale of environmental correlations and dispersal interact in their effects on total synchrony. In every case, there is significant total synchrony or anti-synchrony (relative to the standard errors), despite zero overall correlation in habitat sizes.

The response of total synchrony (mean correlations in population numbers) varied among treatments groups in our experimental design. Two-factor ANOVA showed that the overall effect of the two-level frequency-specific habitat fluctuation factor was highly significant for all three life stages ($p < 0.0001$). The effect of dispersal on total synchrony was not significant for the L-stage and P-stage insects, but was highly significant for the A-stage ($p < 0.0001$). The interaction effect between habitat size and dispersal was not significant for the P-stage and was barely significant for the L-stage ($p = 0.031$), but was highly significant for adults ($p < 0.0001$). Details are in SI-§S6.1.

The corrpectral slope summarised effects of habitat fluctuations and dispersal on the timescale of synchrony (Methods). For the L-stage, the $Low^+/High^-$ habitat regime resulted in

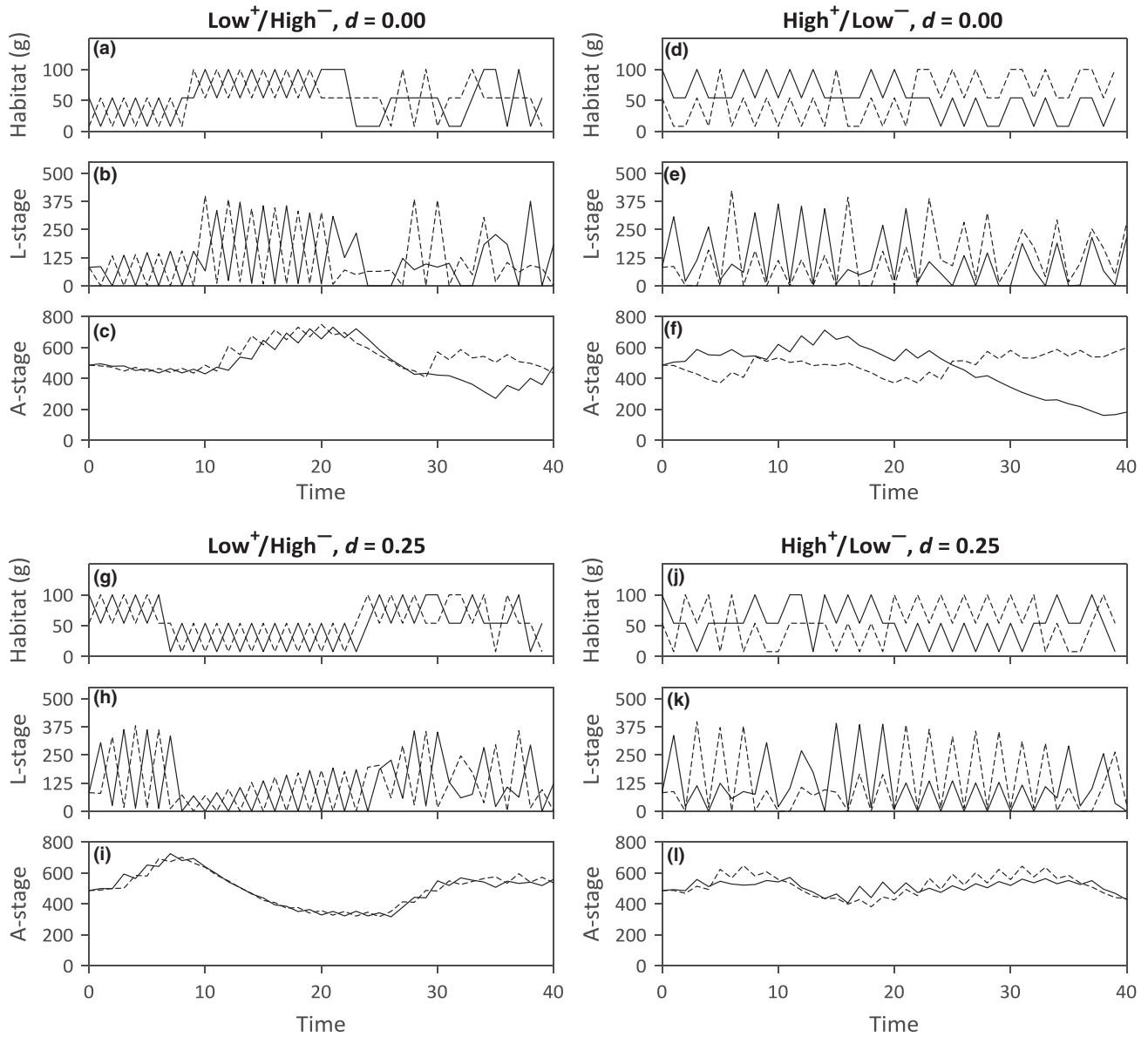


Figure 1 Time series for the random flour volume sequences and the observed L-stage and A-stage numbers. One replicate is shown from each of the four experimental treatment groups. Solid and dashed lines are for the two component populations of the metapopulations. P-stage insects at time t were approximately proportional to L-stage insects at time $t-1$, and so are omitted. Time series for all life stages and replicates appear in SI-§S5.

large negative slopes, whereas the $\text{High}^+/\text{Low}^-$ habitat regime resulted in large positive values (Fig. 4). These differences were highly significant ($p < 0.0001$, two-factor ANOVA). There was no significant overall effect due to dispersal and no significant interaction. For the A-stage, the response of the corrspectral slopes was similar to that of the L-stage, except with dispersal in the $\text{High}^+/\text{Low}^-$ habitat regime. In this treatment, the mean A-stage corrspectral slope was close to zero and there was a highly significant interaction between habitat fluctuations and dispersal ($p < 0.0001$). ANOVA tables are given in SI-§S6.2.

Spectral predictions from linear filter theory

Filter theory was applied to a linearised version of the M-LPA model with the CLS parameter estimates to yield

predictions for the normalised population spectra, $\tilde{S}_w(f)$, and metapopulation corrspectra, $\tilde{C}_w(f)$, for each life-stage and treatment group. Figure 5 shows predictions for the L-stage and A-stage for comparison with experimental results in Fig. 3.

Linear filter theory predicted well the different responses of the immatures and adults to habitat fluctuations. The L-stage was predicted to be mostly sensitive to high-frequency fluctuations as indicated by the concentration of the spectral power at the highest frequencies. The A-stage effectively filtered out high-frequency fluctuations in habitat size, so the spectral power was concentrated at low frequencies. These patterns match well with the observed normalised spectra (Fig. 3). For the A-stage in the $\text{High}^+/\text{Low}^-$ habitat regime with dispersal, the predicted spectrum increases slightly in spectral power at

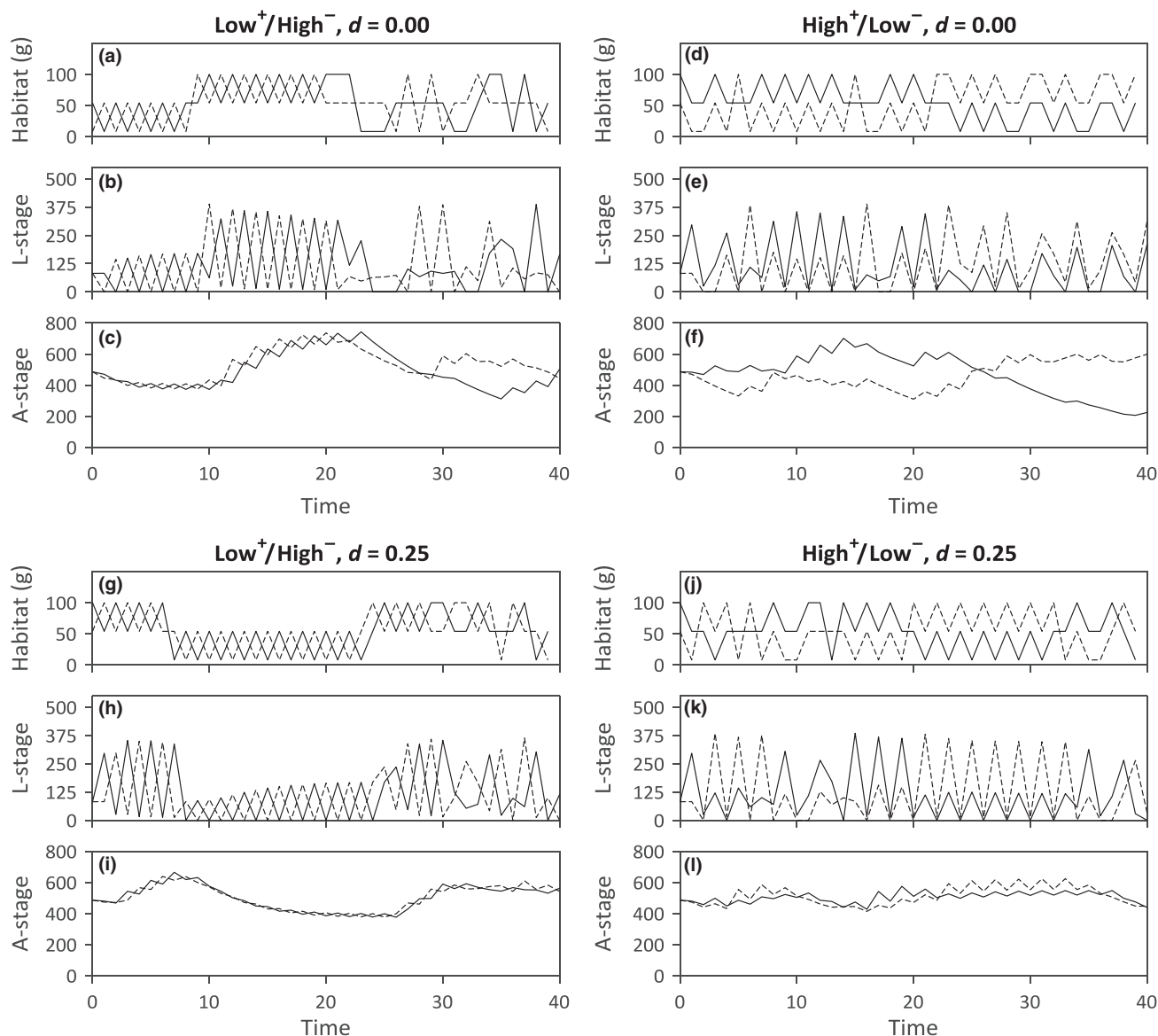


Figure 2 Time series plots for the random flour volume sequences and the L-stage and A-stage numbers predicted using the M-LPA model with experimental initial conditions and CLS parameter estimates. The habitat size sequences are the same as the replicates in Fig. 1. Solid and dashed lines are for the two component populations of the experimental metapopulations. Compare Fig. 2 with Fig. 1. Predicted time series for all life stages and replicates appear in SI-§S5.

high frequencies (Fig. 5q), similar to the response in the experimental data (Fig. 3n).

As predicted by the analysis of the model (8), in the absence of dispersal, a frequency-specific analog of the Moran theorem holds: the population corrspectrum equals the environmental corrspectrum (Fig. 5f, g, j, k). The frequency-specific analog of the Moran theorem does not apply when dispersal is present. Nevertheless, filter theory predicts that the population corrspectra are similar to the environmental corrspectra when dispersal is present, except the population corrspectra are slightly curvilinear (Fig. 5n, o, r), and except for the A-stage in the High⁺/Low⁻ habitat regime (Fig. 5s). Observed corrspectra in Fig. 3 also follow this predicted trend of gradually increasing (decreasing) from a minimum (maximum) value. In fact, the predicted corrspectral slopes should be near either +4 or -4, as observed in the corrspectral slopes in

Fig. 4. For the A-stage in the High⁺/Low⁻ habitat regime with dispersal, agreement between observed and predicted corrspectra is not as good. While linear filter theory predicted correctly that dispersal would have its largest effect on the adult stage in the High⁺/Low⁻ environmental regime and that the corrspectra would be flattened at low frequencies, the level at which the flattening occurs in the experimental data is higher than predicted (Fig. 3p vs. Fig. 5s).

DISCUSSION

Key results

We demonstrated, theoretically and experimentally, that if population growth rates in two locations are influenced by an environmental factor that is correlated through time in the

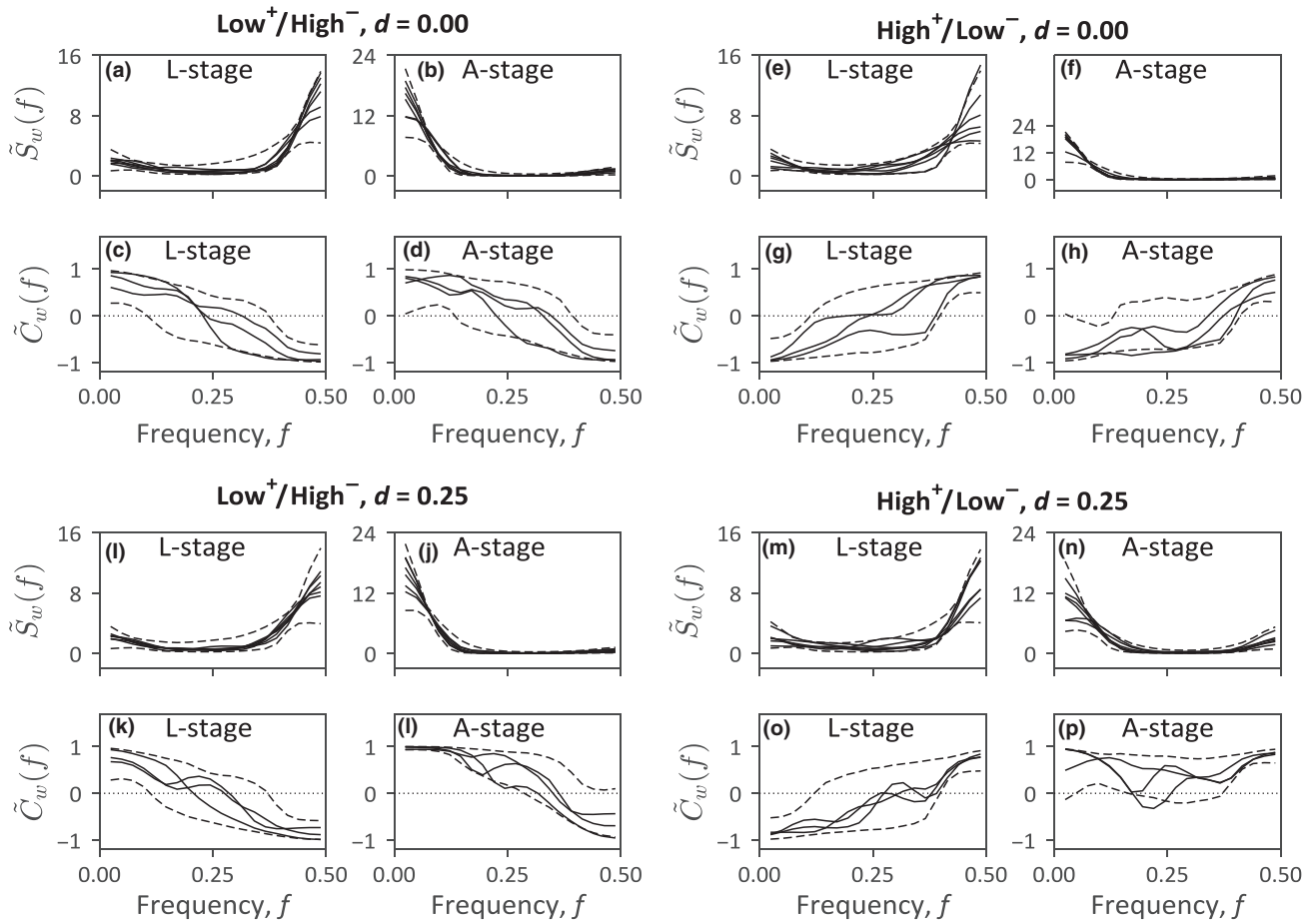


Figure 3 Normalised spectral densities and cospectra for the observed L-stage and A-stage numbers. Each group of four panels is for the different treatment groups as indicated in headers. The plots of the normalised spectra, $\tilde{S}_w(f)$, have six curves because there are two populations for each of the three replicate metapopulations. The plots of the cospectra, $\tilde{C}_w(f)$, have three curves, one for each bivariate population time series from each of the three replicate metapopulations. Dashed curves are 95% confidence intervals based on model simulations with CLS-fitted parameters (Methods).

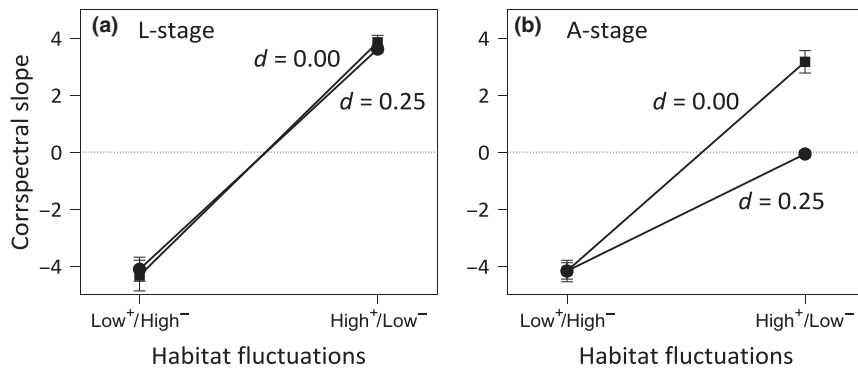


Figure 4 Mean \pm SE of the slopes of the cospectra in Fig. 3 for the (a) L-stage and (b) A-stage.

two locations, then changes in the timescale of the environmental correlation can induce changes in total synchrony and the timescale structure of synchrony. This finding is true even when the autocorrelation structure (spectrum) of the environmental fluctuations in each location and the total correlation between environmental time series are unchanged. In short, spectral properties of environmental correlations influence synchrony.

Dispersal can affect the timescale structure of synchrony. Our theoretical analysis showed that, at each frequency, the population cospectrum is a weighted average of the spectrum and cospectrum of environmental variation; and that the balance of this weighting depends on the level of dispersal (SI-§1.1 eq. 1.17). In the absence of dispersal ($d = 0$), there is no balance: the spectrum and cospectrum of the environmental noise have no effect on the cospectrum and spectrum,

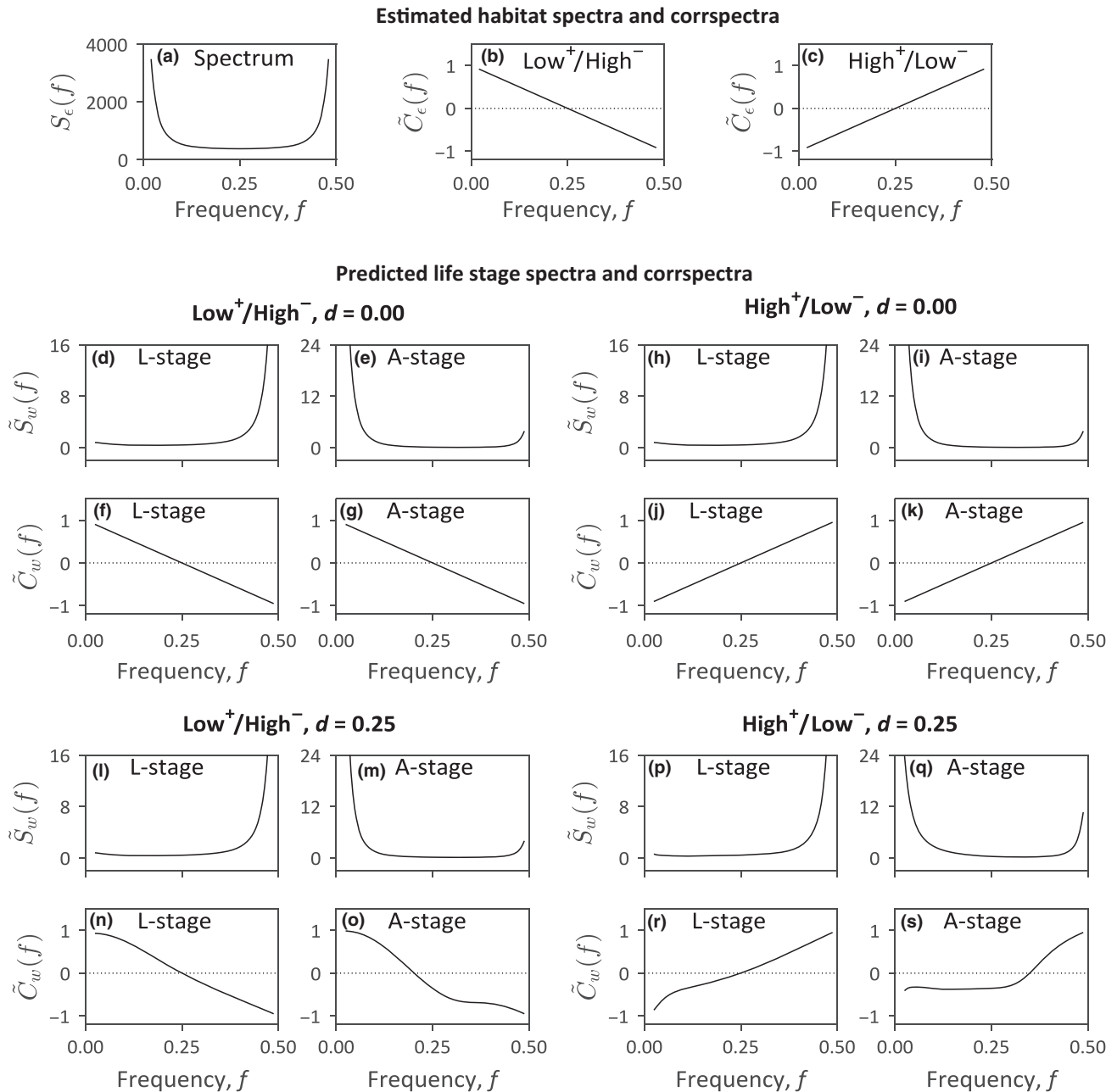


Figure 5 Predicted spectra and corrspectra for the habitat fluctuations and L-stage and A-stage population numbers. Panels (a)–(c) are theoretical habitat spectra and corrspectra (Methods). Remaining panels, laid out as in Fig. 3, are predicted normalised spectra and corrspectra for the L-stage and A-stage based on linear filter theory applied to the linearised M-LPA model (Methods). Compare Fig. 5 with Fig. 3.

respectively, of the population trajectories (SI-§S1.1 eq. 1.26, 1.28). As dispersal increases towards its maximum value ($d = 0.5$), the weighting becomes equal: the population spectrum and cospectrum converge as one might expect for two well-mixed populations.

The timescale-specificity of this weighting varies with the dynamic stability properties of the population, resulting in a three-way interaction among dispersal, the timescale of environmental stochasticity, and population stability in their effects on the timescale of synchrony. Our experiment provides an example. The timescale of the synchrony of adult numbers is strongly affected by dispersal, but only in the

metapopulations with a High⁺/Low⁻ habitat regime (Fig. 3). Simulations using nonlinear metapopulation models support these conclusions (Danielian 2016).

Our theoretical results also provide a timescale-specific extension of the Moran theorem (Moran 1953) on the ability of correlated environmental variation to synchronise population dynamics. Using a pair of linear second-order autoregressive equations with correlated white noise, Moran showed that the correlation between the population variables will equal the correlation between the environmental variables, thus providing a mechanism for synchrony. Our theoretical results showed that, in the absence of dispersal and when

there is a timescale structure to the environmental covariance, the corrspectrum of the populations will equal the corrspectrum of the environmental noise at every frequency, that is, $\tilde{C}_w(f) = \tilde{C}_e(f)$. Our experiment provided a case study. Figure 5 showed that the corrspectra of the habitat fluctuations equaled the predicted corrspectra for L-stage and A-stage in the absence of dispersal ($d = 0$), and the experimental results supported this conclusion (Fig. 3). This extension of Moran's theorem could have practical value: one may be able to compare the corrspectra of environmental variables and population time series to infer the extent to which the Moran effect drives synchrony.

Practical implications

Our results may have practical implications for conservation biology and natural resource management. The timescale of environmental noise has implications for the risk of extinction of single populations through its effect on population dynamics (Ripa & Lundberg 1996; Heino 1998; Heino *et al.* 2000; Schwager *et al.* 2006; García-Carreras & Reuman 2011). In general, theoretical analyses from unstructured population models suggest that environmental spectra that are shifted toward longer timescales increase extinction risk for slowly growing populations and decrease extinction risk for rapidly growing populations (García-Carreras & Reuman 2011). Other studies have argued that an increase in synchrony can increase the extinction risk of metapopulations (Harrison & Quinn 1989; Heino *et al.* 1997; Earn *et al.* 2000). Recent simulations using metapopulations with dynamics based on the Ricker model suggest that reddened environmental corrspectra will have a similar effect on the risk of metapopulation extinction (Danielian 2016). Our results help identify situations where shifts in the timescale of environmental correlations may affect the extinction of natural populations. Shifts in the timescale and strength of environmental correlations have been connected to impacts on pests (Sheppard *et al.* 2016) and birds (Koenig & Liebhold 2016).

We used methods based on Fourier analysis, which assume the modelled system is a stationary stochastic process. This assumption may not be valid for real-world data. Methods based on wavelets are an alternative. Wavelet coherence cross-spectra provide a measure of the correlation between two time series as a function of both time and frequency (Torrence & Compo 1998; Addison 2016), and can be averaged over time to yield a global wavelet spectrum.

Our theoretical and experimental results suggest that linear filter theory can be a valuable tool to study the timescale of synchrony. Although this theory is based on linear population models, it described our laboratory system successfully. The strongly nonlinear nature of the LPA model has been exploited to study population phenomena such as cycles, invariant loops, resonance effects, and chaos (Cushing *et al.* 2002; Costantino *et al.* 2005). Furthermore, although the linearisation of the M-LPA model requires the assumption of a stable equilibrium and weak noise, our random habitat treatment involved large changes in flour volumes, resulting in large changes in population numbers, especially in the immature life stages (Fig. 1), but predictions of linear filter theory were still largely supported experimentally. The accuracy, in

this example, of linear filter theory should encourage evaluation of its usefulness in other studies.

ACKNOWLEDGMENTS

RAD, RFC, and JEC were supported by US National Science Foundation (NSF) grant DMS-1225529. DCR was supported by the James S. McDonnell Foundation, the University of Kansas, and NSF grants 1442595 and 1714195. RAD thanks Richard M. Murray at the California Institute of Technology for his hospitality while portions of this work were completed there. DCR thanks Lawrence W. Sheppard for helpful discussions. JEC thanks Roseanne Benjamin for help.

AUTHOR CONTRIBUTIONS

DCR and RFC developed the experimental design with input from RAD and JEC. RFC carried out the experiment. DCR derived the general mathematical results for the effects of timescale-specific noise on population synchrony. RAD derived the application of linear filter theory to the *Tribolium* metapopulation model and conducted the data analyses and model simulations. RAD wrote a first draft of the manuscript, which was revised with input from DCR, RFC, and JEC.

DATA ACCESSIBILITY STATEMENT

The data supporting the results are archived at <https://doi.org/10.5061/dryad.8024p3h>.

REFERENCES

- Abbott, K.C. (2007). Does the pattern of population synchrony through space reveal if the Moran effect is acting? *Oikos*, 116, 903–912.
- Addison, P.S. (2016). *The illustrated wavelet transform handbook: Introductory theory and applications in science, engineering, medicine and finance*, 2nd ed. CRC Press, Boca Raton.
- Benoît, H.P., McCauley, E. & Post, J.R. (1998). Testing the demographic consequences of cannibalism in *Tribolium confusum*. *Ecology*, 79, 2839–2851.
- Benton, T.G., Lapsley, C.T. & Beckerman, A.P. (2001). Population synchrony and environmental variation: an experimental demonstration. *Ecol. Lett.*, 4, 236–243.
- Benton, T.G., Lapsley, C.T. & Beckerman, A.P. (2002). The population response to environmental noise: population size, variance and correlation in an experimental system. *J. Anim. Ecol.*, 71, 320–332.
- Bjørnstad, O.N. & Falck, W. (2001). Nonparametric spatial covariance functions: estimation and testing. *Environ. Ecol. Stat.*, 8, 53–70.
- Bjørnstad, O.N., Ims, R.A. & Lambin, X. (1999). Spatial population dynamics: analyzing patterns and processes of population synchrony. *Trends Ecol. Evol.*, 14, 427–432.
- Bjørnstad, O.N., Liebhold, A.M. & Johnson, D.M. (2008). Transient synchronization following invasion: revisiting Moran's model and a case study. *Popul. Ecol.*, 50, 379–389.
- Buonaccorsi, J.P., Elkinton, J.S., Evans, S.R. & Liebhold, A.M. (2001). Measuring and testing for spatial synchrony. *Ecology*, 82, 1668–1679.
- Chevalier, M., Laffaille, P. & Grenouillet, G. (2014). Spatial synchrony in stream fish populations: influence of species traits. *Ecography*, 37, 960–968.
- Cohen, J.E., Newman, C.M., Cohen, A.E., Petchey, O.L. & Gonzalez, A. (1999). Spectral mimicry: a method of synthesizing matching time series with different Fourier spectra. *Circ. Syst. Signal Pr.*, 18, 431–442.

- Costantino, R.F., Cushing, J.M., Dennis, B. & Desharnais, R.A. (1995). Experimentally induced transitions in the dynamic behaviour of insect populations. *Nature*, 375, 227–230.
- Costantino, R.F., Desharnais, R.A., Cushing, J.M. & Dennis, B. (1997). Chaotic dynamics in an insect population. *Science*, 275, 389–391.
- Costantino, R.F., Cushing, J.M., Dennis, B., Desharnais, R.A. & Henson, S.M. (1998). Resonant population cycles in temporally fluctuating habitats. *B. Math. Biol.*, 60, 247–273.
- Costantino, R.F., Desharnais, R.A., Cushing, J.M., Dennis, B., Henson, S.M. & King, A.A. (2005). Nonlinear stochastic population dynamics: the flour beetle *Tribolium* as an effective tool of discovery. *Adv. Ecol. Res.*, 37, 101–141.
- Cushing, J.M., Costantino, R.F., Dennis, B., Desharnais, R.A. & Henson, S.M. (2002). *Chaos in ecology: experimental nonlinear dynamics*. Academic Press, San Diego.
- Danielian, S. (2016). *The effects of environmental noise and dispersal on ecological extinction and the spectral properties of metapopulations*. Master's thesis, California State University, Los Angeles.
- Defriez, E.J., Sheppard, L.W., Reid, P.C. & Reuman, D.C. (2016). Climate change-related regime shifts have altered spatial synchrony of plankton dynamics in the North Sea. *Global Change Biol.*, 22, 2069–2080.
- Defriez, E.J. & Reuman, D.C. (2017a). A global geography of synchrony for marine phytoplankton. *Global Ecol. Biogeogr.*, 26, 867–877.
- Defriez, E.J. & Reuman, D.C. (2017b). A global geography of synchrony for terrestrial vegetation. *Global Ecol. Biogeogr.*, 26, 878–888.
- Dennis, B., Desharnais, R.A., Cushing, J.M. & Costantino, R.F. (1995). Nonlinear demographic dynamics: mathematical models, statistical methods, and biological experiments. *Ecol. Monogr.*, 65, 261–282.
- Dennis, B., Desharnais, R.A., Cushing, J.M., Henson, S.M. & Costantino, R.F. (2001). Estimating chaos and complex dynamics in an insect population. *Ecol. Monogr.*, 71, 277–303.
- Desharnais, R.A. (2005). *Population dynamics and laboratory ecology*. Elsevier, San Diego.
- Desharnais, R.A. & Liu, L. (1987). Stable demographic limit cycles in laboratory populations of *Tribolium castaneum*. *J. Anim. Ecol.*, 56, 885–906.
- Desharnais, R.A., Costantino, R.F., Cushing, J.M., Henson, S.M., Dennis, B. & King, A.A. (2006). Experimental support of the scaling rule for demographic stochasticity. *Ecol. Lett.*, 9, 537–547.
- Dey, S. & Joshi, A. (2006). Stability via asynchrony in *Drosophila* metapopulations with low migration rates. *Science*, 312, 434–6.
- Duncan, A.B., Gonzalez, A. & Kaltz, O. (2015). Dispersal, environmental forcing, and parasites combine to affect metapopulation synchrony and stability. *Ecology*, 96, 284–290.
- Earn, D.J.D., Rohani, P. & Grenfell, B.T. (1998). Persistence, chaos and synchrony in ecology and epidemiology. *Proc. Roy. Soc. Lond. B*, 265, 7–10.
- Earn, D.J.D., Levin, S.A. & Rohani, P. (2000). Coherence and conservation. *Science*, 290, 1360–1364.
- Fontaine, C. & Gonzalez, A. (2005). Population synchrony induced by resource fluctuations and dispersal in an aquatic microcosm. *Ecology*, 86, 1463–1471.
- Fox, J.W., Vasseur, D.A., Hausch, S. & Roberts, J. (2011). Phase locking, the Moran effect and distance decay of synchrony: experimental tests in a model system. *Ecol. Lett.*, 14, 163–168.
- García-Carreras, B. & Reuman, D.C. (2011). An empirical link between the spectral colour of climate and the spectral colour of field populations in the context of climate change. *J. Anim. Ecol.*, 80, 1042–1048.
- Grenfell, B.T., Bjørnstad, O.N. & Kappey, J. (2001). Travelling waves and spatial hierarchies in measles epidemics. *Nature*, 414, 716–723.
- Harrison, S. & Quinn, J.F. (1989). Correlated environments and the persistence of metapopulations. *Oikos*, 56, 293–298.
- Haydon, D. & Steen, H. (1997). The effects of large- and small-scale random events on the synchrony of metapopulation dynamics: a theoretical analysis. *Proc. Roy. Soc. Lond. B*, 264, 1375–1381.
- Heino, M. (1998). Noise colour, synchrony and extinctions in spatially structured populations. *Oikos*, 83, 368–375.
- Heino, M., Kaitala, V., Ranta, E. & Lindstrom, J. (1997). Synchronous dynamics and rates of extinction in spatially structured populations. *Proc. Roy. Soc. Lond. B*, 264, 481–486.
- Heino, M., Ripa, J. & Kaitala, V. (2000). Extinction risk under coloured environmental noise. *Ecography*, 23, 177–184.
- Henson, S.M., Costantino, R.F., Desharnais, R.A., Cushing, J.M. & Dennis, B. (2002). Basins of attraction: population dynamics with two stable 4-cycles. *Oikos*, 98, 17–24.
- Hudson, P.J. & Cattadori, I.M. (1999). The Moran effect: a cause of population synchrony. *Trends Ecol. Evol.*, 14, 1–2.
- Jessup, C.M., Kassen, R., Forde, S.E., Kerr, B., Buckling, A., Rainey, P.B. *et al.* (2004). Big questions, small worlds: microbial model systems in ecology. *Trends Ecol. Evol.*, 19, 189–197.
- Kahilainen, A., van Nouhuys, S., Schulz, T. & Saastamoinen, M. (2018). Metapopulation dynamics in a changing climate: increasing spatial synchrony in weather conditions drives metapopulation synchrony of a butterfly inhabiting a fragmented landscape. *Glob. Change Biol.*, 24, 4316–4329. <https://doi.org/10.1111/gcb.14280>.
- Keitt, T.H. (2008). Coherent ecological dynamics induced by large-scale disturbance. *Nature*, 454, 331.
- Kendall, B.E., Bjørnstad, O.N., Bascompte, J., Keitt, T.H. & Fagan, W.F. (2000). Dispersal, environmental correlation, and spatial synchrony in population dynamics. *Am. Nat.*, 155, 628–636.
- Koenig, W.D. & Liebhold, A.M. (2016). Temporally increasing spatial synchrony of North American temperature and bird populations. *Nat. Clim. Change*, 6, 614–617.
- Liebhold, A., Koenig, W.D. & Bjørnstad, O.N. (2004). Spatial synchrony in population dynamics. *Annu. Rev. Ecol. Evol. S.*, 35, 467–490.
- Lima-Ribeiro, M.S., Moura, I.O., Pinto, M.P., Nabout, J.C., Melo, T.L., Costa, S.S. *et al.* (2007). Evidences of Moran effect in the population synchrony: a demonstration in experimental microcosm. *Neotrop. Entomol.*, 36, 662–669.
- Martin, A.E., Pearce-Higgins, J.W. & Fahrig, L. (2017). The spatial scale of time-lagged population synchrony increases with species dispersal distance. *Global Ecol. Biogeogr.*, 26, 1201–1210.
- Massie, T.M., Weithoff, G., Kuckländer, N., Gaedke, U. & Blasius, B. (2015). Enhanced Moran effect by spatial variation in environmental autocorrelation. *Nat. Commun.*, 6, 5993.
- Moran, P.A.P. (1953). The statistical analysis of the Canadian lynx cycle II: synchronization and meteorology. *Aust. J. Zool.*, 1, 291–298.
- Myers, J.H. (1990). Population-cycles of western tent caterpillars—experimental introductions and synchrony of fluctuations. *Ecology*, 71, 986–995.
- Myers, J.H. (1998). Synchrony in outbreaks of forest Lepidoptera: a possible example of the Moran effect. *Ecology*, 79, 1111–1117.
- Porter, J.H., Parry, M.L. & Carter, T.R. (1991). The potential effects of climatic change on agricultural insect pests. *Agr. Forest Meteorol.*, 57, 221–240.
- Post, E. & Forchhammer, M.C. (2004). Spatial synchrony of local populations has increased in association with the recent Northern Hemisphere climate trend. *Proc. Natl Acad. Sci. USA*, 101, 9286–9290.
- Ranta, E., Kaitala, V., Lindstrom, J. & Linden, H. (1995). Synchrony in population dynamics. *Proc. Roy. Soc. Lond. B*, 262, 113–118.
- Ranta, E., Kaitala, V., Lindstrom, J. & Helle, E. (1997). The Moran effect and synchrony in population dynamics. *Oikos*, 78, 136–142.
- Reuman, D.C., Desharnais, R.A., Costantino, R.F., Ahmad, O.S. & Cohen, J.E. (2006). Power spectra reveal the influence of stochasticity on nonlinear population dynamics. *Proc. Natl Acad. Sci. USA*, 103, 18860–18865.
- Reuman, D.C., Costantino, R.F., Desharnais, R.A. & Cohen, J.E. (2008). Colour of environmental noise affects the nonlinear dynamics of cycling, stage-structured populations. *Ecol. Lett.*, 11, 820–830.
- Ripa, J. (2000). Analysing the Moran effect and dispersal: their significance and interaction in synchronous population dynamics. *Oikos*, 89, 175–187.
- Ripa, J. & Lundberg, P. (1996). Noise colour and the risk of population extinctions. *Proc. Roy. Soc. Lond. B*, 263, 1751–1753.

- Ripa, J. & Ranta, E. (2007). Biological filtering of correlated environments: towards a generalised Moran theorem. *Oikos*, 116, 783–792.
- Schwager, M., Johst, K. & Jeltsch, F. (2006). Does red noise increase or decrease extinction risk? Single extreme events versus series of unfavorable conditions. *Am. Nat.*, 167, 879–888.
- Sheppard, L.W., Bell, J.R., Harrington, R. & Reuman, D.C. (2016). Changes in large-scale climate alter spatial synchrony of aphid pests. *Nat. Clim. Change*, 6, 610–613.
- Shestakova, T.A., Gutiérrez, E., Kiryanov, A.V., Camarero, J.J., Génova, M., Knorre, A.A. *et al.* (2016). Forests synchronize their growth in contrasting Eurasian regions in response to climate warming. *Proc. Natl Acad. Sci. USA*, 113, 662–667.
- Torrence, C. & Compo, G.P. (1998). A practical guide to wavelet analysis. *B. Am. Meteorol. Soc.*, 79, 61–78.
- Vasseur, D.A. & Fox, J.W. (2009). Phase-locking and environmental fluctuations generate synchrony in a predator-prey community. *Nature*, 460, 1007.
- Vasseur, D.A. & Gaedke, U. (2007). Spectral analysis unmask synchronous and compensatory dynamics in plankton communities. *Ecology*, 88, 2058–2071.
- Vogwill, T., Fenton, A. & Brockhurst, M.A. (2009). Dispersal and natural enemies interact to drive spatial synchrony and decrease stability in patchy populations. *Ecol. Lett.*, 12, 1194–1200.

SUPPORTING INFORMATION

Additional supporting information may be found online in the Supporting Information section at the end of the article.

Editor, David Vasseur

Manuscript received 19 March 2018

First decision made 4 May 2018

Second decision made 29 July 2018

Manuscript accepted 16 August 2018